# Origin and orientation of the electric field gradient in ordered FeNi

Diana Guenzburger and D. E. Ellis*
*Centro Brasileiro de Pesquisas Físicas, Rua Dr. Xavier Sigaud, 150-22290, Rio de Janeiro, RJ, Brazil*
(Received 14 April 1987)

The electronic structure of tetrataenite, the ordered phase of FeNi, has been studied in the molecular cluster approximation using local-density theory. Clusters containing 13 and 19 atoms were embedded in the fcc host lattice, and spin-unrestricted potentials were iterated to self-consistency. Local moments, magnetic hyperfine fields, and electric field gradients (EFG) at the iron sites were determined for comparison with experiment. The orientation of the EFG principal axis is found to be parallel to the superstructure $c$ axis.

## I. INTRODUCTION

Iron-nickel alloys $Ni_xFe_{1-x}$ exist over the entire composition range[1-7] and, with various added elements such as Cr and C, are of considerable importance for structural applications where high strength and resistance to corrosion are required. Both bcc and fcc phases are found, with fcc disordered phases predominating for $x \geq 0.4$. Except for notable cases such as the ordered $Ni_3Fe$ and NiFe structures, random occupancy of lattice sites by either type of atom is presumed. At low Ni concentrations, the fcc phase can be stabilized by quenching or phosphorous doping, and an antiferromagnetic structure is observed at low temperatures. The Invar alloys, well known for their low thermal expansion, span the antiferromagnetic to ferromagnetic transition region $0.25 \lesssim x \lesssim 0.35$.

The 50-50 composition forms an ordered compound with the CuAu structure, consisting of alternating layers of Ni and Fe on an fcc lattice. This superlattice compound is found in certain meteorites, and is known as tetrataenite.[1,2] It has also been obtained by neutron irradiation of the disordered FeNi alloy.[3] The disordered phase is most stable for $T_c \geq 590$ K, and the diffusion rate for $T < T_c$ is very low. Observation of the relative fraction of tetrataenite in ferronickel meteorites permits useful estimates of the rate of cooling, of the order of 1–2 K per million years. The ordered compound is resistant to corrosion, meteoritic samples in the form of lamallae being obtained by dissolving the host Fe-Ni matrix in acid.

A small tetragonal distortion of the fcc structure has been observed by x-ray diffraction.[1] Magnetic hyperfine fields ($H_f$) and electric field gradients (EFG's) at Fe sites have been obtained by several groups, using Mössbauer spectroscopy.[5-7] In principle, the use of external magnetic fields in the Mössbauer experiment permits determination of the *sign* of the EFG as well as its magnitude. In addition, the orientation of the principal EFG axis relative to the internal magnetic field direction can also be found. The present work was motivated in part by a desire to understand the origins of the observed EFG, and to resolve its orientation relative to that of the internal magnetic field. The sign of the theoretical EFG is determined unambiguously here, and related to the Ni—Fe versus Fe—Fe bonding interactions.

## II. ELECTRONIC STRUCTURE CALCULATIONS

### A. Theoretical method

Local-density self-consistent field models of electronic structure have proved to be highly successful in describing properties of transition metals and intermetallic compounds. Both band structure and molecular cluster techniques have been developed as first principles tools using a linear combination of atomic orbitals (LCAO) variational approach[8] which is well suited to atomistic chemical interpretations of charge and spin densities as well as spectroscopic properties. Band-structure methods and cluster models for a periodic system tend to the same limit as the cluster size increases, and evidence has gradually accumulated that 3–4 shells of neighbors is sufficient to represent most properties of a particular atomic environment. In treating alloy properties, where local order may be a dominant factor rather than long-range periodicity, representation of the system by small embedded clusters is not only computationally attractive but also physically reasonable.

We have calculated the electronic structure of clusters representing the 50-50 FeNi ordered alloy. We considered both a 13-atom cluster and a 19-atom cluster (Fig. 1), the latter to explore the effect of cluster size. In the mineral tetrataenite,[1,2] which has CuAu structure, each Fe atom is surrounded by eight Ni and four Fe nearest neighbors (NN), with local symmetry $D_{4h}$, as seen in Fig. 1. The second shell of neighbors (NNN), included in the 19-atom cluster, is made up of six Fe atoms, forming an octahedron around the Fe atom at the center of the cluster. In Table I are given the interatomic distances used in the calculations.

The electronic structure for these clusters was obtained with the discrete variational (DV) method[8] in the local exchange approximation.[9] Self-consistent one-electron wave functions were derived by solving approximately the equation

 

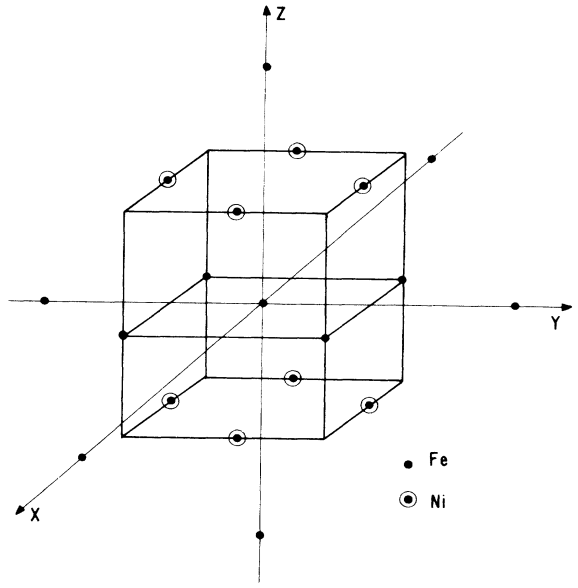


FIG. 1. 19-atom cluster representing the FeNi 50-50 alloy.

$$(h_\sigma-\varepsilon_{i\sigma})\phi_{i\sigma}=\left[-\frac{\nabla^2}{2}+V_{\text{Coul}}+V_x^\sigma-\varepsilon_{i\sigma}\right]\phi_{i\sigma}=0\ , \tag{1}$$

where the one-electron Hamiltonian (in Hartree atomic units) consists of a kinetic energy term, a Coulomb potential-energy term which includes electron-nuclei and electron-electron interactions, and an exchange term which may be expressed as

$$V_x^\sigma(\mathbf{r})=-3\alpha\left[\frac{3}{4\pi}\rho_\sigma\right]^{1/3}\ , \tag{2}$$

and which may be different for each spin $\sigma$. $V_x^\sigma$ is thus a function of the electronic spin density $\rho_\sigma(\mathbf{r})$ defined as

$$\rho_\sigma(\mathbf{r})=\sum_i n_{i\sigma}\,|\,\phi_{i\sigma}(\mathbf{r})\,|^2 \tag{3}$$

and $\alpha=\frac{2}{3}$.[9] Here $n_{i\sigma}$ is the occupation of spin orbital $\phi_{i\sigma}$.

The cluster molecular orbitals $\phi_i$ are expanded over a basis of numerical atomic orbitals, which may include both occupied and vacant orbitals for greater variational freedom. One then obtains a set of secular equations

$$([H]-[E][S])[C]=0\ , \tag{4}$$

TABLE I. Interatomic distances in FeNi ordered phase (Ref. 1).

| Bond distance (Å) | |
|---|---|
| Fe-Fe (first neighbor): | 2.53 |
| Fe-Ni: | 2.53 |
| Fe-Fe (second neibhbor): | 3.58 |

where $[C]$ is the matrix of the coefficients of the expansion, and $[H]$ and $[S]$ are the energy and overlap matrixes, respectively. In the DV method, all the matrix elements in Eq. (4) are calculated by numerical integration; in the valence region, the pseudorandom diophantine integration method[8] is used, and in the core region a precise polynomial integration is performed[10] which is essential for the accurate evaluation of hyperfine interactions.

In order to better represent the solid by the clusters, these are "embedded" in the potential field of several shells of surrounding atoms.[11] The core-region potential of each exterior atom is truncated, to simulate Pauli exclusion effects.

The quadrupole splitting $\Delta_{EQ}$ of the $I=\frac{3}{2}$ nuclear $\gamma$ resonance line of $^{57}$Fe, when an internal magnetic field is present, may be expressed as[12]

$$\Delta_{EQ}=\tfrac{1}{2}eV_{zz}Q\left[\frac{3\cos^2\theta-1}{2}\right]\ , \tag{5}$$

where $\theta$ is the angle between the direction of the magnetic field and the principal axis of the field gradient. $\theta$ cannot be determined from a single Mössbauer experiment, an independent measurement being necessary. On the other hand, one may calculate the principal component of the field gradient tensor $V_{zz}$ using the expression[12] (in a.u.)

$$V_{zz}=\sum_k Z_k\frac{3z_k^2-r_k^2}{r_k^5}-\sum_{i,\sigma}n_{i\sigma}\left\langle\phi_{i\sigma}\left|\frac{3z^2-r^2}{r^5}\right|\phi_{i\sigma}\right\rangle\ , \tag{6}$$

where the first term represents the contribution of the surrounding nuclei of atomic number $Z_k$ (or the nuclei shielded by the core electrons, in the case of a "frozen core" approximation). The second term is the electronic contribution, and represents a sum over the contributions of occupied spin orbitals $\phi_{i\sigma}$, with occupation $n_{i\sigma}$.

When the spin orbitals in the second term of Eq. (6) are expanded in the linear combination of atomic orbitals, one-center and multiple-center terms result. The first are calculated analytically, using the coefficients of Eq. (4), and the latter are evaluated using special techniques of numerical integration.[13,14]

### B. Quadrupole splitting of $^{57}$Fe in FeNi

In Table II are given the calculated values of the components of $V_{zz}$ of the Fe atom at the center of the clusters, as well as its total value. *It is seen that the calculated $V_{zz}$ is positive.* This result indicates that $\theta=0°$ (and not $\theta=90°$), that is, the axis of $V_{zz}$ is parallel to the axis of the internal magnetic field, since the measured $\Delta_{EQ}$ is also positive. This also implies that the internal magnetic field is oriented perpendicular to the lamallae; i.e., along the $z$ axis of Fig. 1. The quadrupole moment $Q$ of $^{57}$Fe in the excited state $I=\frac{3}{2}$ has been estimated to be of the order of $+0.2$.[12,15] Equation (5) now reduces to

TABLE II. Calculated value of $V_{zz}$ and its components (in a.u.). The nuclear contribution is + 0.073.

| | 13-atom cluster | 19-atom cluster |
|---|---|---|
| One center, spin up | + 0.026 | + 0.149 |
| One center, spin down | + 0.350 | + 0.407 |
| Two and three center, spin up | + 0.012 | + 0.013 |
| Two and three center, spin down | + 0.012 | + 0.010 |
| Total $V_{zz}$ | + 0.473 | + 0.652 |
| $\Delta_{EQ}$ (mm/s)[a] | + 0.74 | + 1.03 |

[a]According to Eq. (7). Value of $Q$ from Ref. 15 ($Q = 0.156$ b).

$$\Delta_{EQ} = \tfrac{1}{2} V_{zz} eQ \ , \tag{7}$$

since the angular term in large parentheses is equal to $+1$ for $\theta = 0$.

Of all the contributions given in Table II, it can be seen that it is the one-center spin-down term that determines the sign and, to a great extent, the magnitude of $V_{zz}$. The nuclear and multiple-center terms are all very small, and the one-center spin-up adds to a small number also, since the spin-up valence states at the site of the central Fe atom are all occupied (see the density of states diagrams, Figs. 2 and 3).

From the results given in Table II it is also seen that increasing the number of atoms in the cluster from 13 to 19 does not have a major effect on $V_{zz}$; this increases our confidence in the stability of the results regarding cluster size.

To better understand the origin of the positive contribution to $V_{zz}$ given by the spin-down orbitals, we have broken up this contribution into its components according to the symmetry group $D_{4h}$. These are given in Table III.

On examining these numbers, it may be noticed that the $a_{1g}$ orbitals give a contribution which is negative, and of about the same magnitude as the $b_{1g}$. For the central Fe atom, the $3d_{z^2}$ orbital transforms as $a_{1g}$, and is pointed along the $z$ axis, towards two of the Fe atoms in the second shell of neighbors. The $3d_{x^2-y^2}$ transforms as $b_{1g}$, and points, in the $x$ and $y$ directions, also towards Fe atoms in the second shell of neighbors. The contributions of these two orbitals almost cancel each other. As seen in Table IV, the six Fe atoms in this shell are almost equivalent, from the point of view of chemical environment; in fact, the Mulliken populations of the orbitals of the axial and equatorial next-nearest-neighbor Fe atoms are very similar. This explains the almost null one-center contribution to $V_{zz}$ coming from the $3d_{z^2}$ and $3d_{x^2-y^2}$ pair of the central Fe.

The orbitals $3d_{xy}$, $3d_{xz}$, and $3d_{yz}$ of central Fe, which are degenerate in octahedral or cubic symmetries, decompose into $b_{2g}(3d_{xy})$ and $e_g(3d_{xz}, 3d_{yz})$ in $D_{4h}$ symmetry. The $b_{2g}$ orbital gives a large positive contribution to $V_{zz}$, which is only canceled in part by the negative contributions of the $e_g$ pair. The explanation for this lies again in the electronic environment which the electrons in these orbitals experience. The $3d_{xy}$ orbital points towards the four Fe atoms in the $xy$ plane. On the other hand, the $3d_{xz}$ and $3d_{yz}$ point toward the Ni atoms. The latter withdraw a small amount of charge from the Fe atoms, as seen in Table IV. In fact, estimates of electronegativity values[16] show that Ni attracts electronic charge in a metallic bond more than Fe does. This explains the reduction of the one-center spin-down contribution to $V_{zz}$ due to the $e_g$ orbitals. The resulting $V_{zz}$ due to all $3d$ orbitals is thus positive. We also give in Table III the contributions of the $4p$ orbitals. These are seen to be small, and largely cancel one another.

To have additional proof for the origin of the positive $V_{zz}$, we have made a calculation for a cluster in which the Ni atoms above the central plane in Fig. 1 have been substituted by Fe atoms, and the four Fe atoms surrounding the central atom in the $x$-$y$ plane were in turn replaced by Ni. The resulting $V_{zz}$ which was obtained was *negative* ($-0.23$ a.u.), showing that indeed the position of the Ni atoms in the ordered FeNi alloy, to which point the $3d_{xz}$ and $3d_{yz}$ orbitals of the Fe atoms, is what determines the sign of $V_{zz}$.

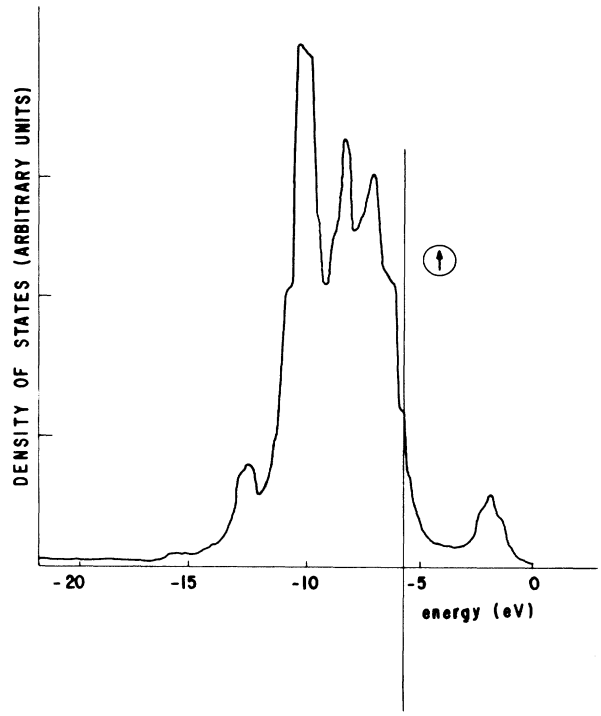


FIG. 2. $3d$, $4s$, and $4p$ density of states at the central Fe atom for spin up.

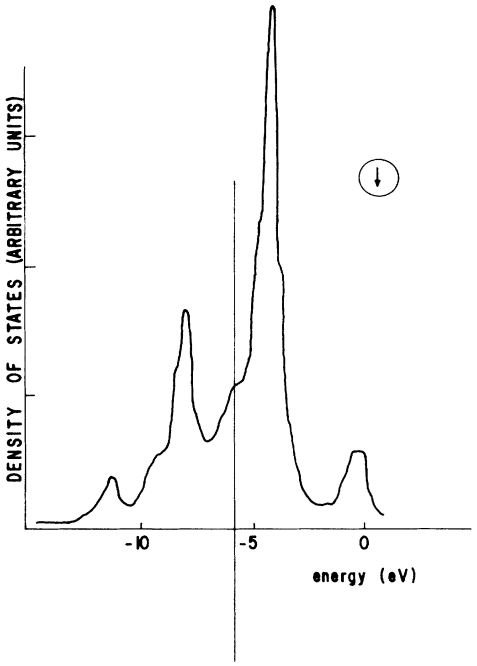


FIG. 3. $3d$, $4s$, and $4p$ density of states at the central Fe atom for spin down.

In summary, the sign that we obtained for $V_{zz}$ is coherent with what may be expected from considerations of the bonding between each Fe atom and its neighbors.

### C. Magnetic properties

In Table IV are given the Mulliken populations of the atoms in the cluster, as well as the charges and magnetic moments. In these spin-polarized calculations, the difference between the spin-up and spin-down total populations on a given atom may be used to define the local magnetic moment in Bohr magnetons.

We notice in Table IV that all atoms have increased $3d$ populations, as compared to the free-atom configuration. This result is consistent with band structure and cluster calculations for a variety of transition metals and their alloys. The $4s$ population is decreased, and some $4p$ charge appears. Overall, the NNN atoms present more atomiclike character than the central atom, which, by its position in the cluster, better represents a bulk atom.[14,17] The rather large positive charge on the central atom is essentially a cluster effect; the population analysis accentuates the special role of the basis attached to the central atom. A volume integration generally yields smaller charge differences, due to the different allocation of diffuse charge. In fact, the finite groups of atoms considered to represent the solid show an imbalance of the charge distribution among similar atoms, due to truncation of the external atoms bonds.

TABLE III. One-center spin-down contributions to $V_{zz}$ (in a.u.) for the 19-atom cluster.

| | |
|---|---|
| $3d$ | |
| $a_{1g}(3d_{z^2})$ | $-0.680$ |
| $b_{1g}(3d_{x^2-y^2})$ | $+0.681$ |
| $b_{2g}(3d_{xy})$ | $+1.005$ |
| $e_g(3d_{xz}+3d_{yz})$ | $-0.646$ |
| $4p$ | |
| $a_{2u}(4p_z)$ | $-0.120$ |
| $e_u(4p_x+4p_y)$ | $+0.171$ |

The calculated magnetic moments on the Fe atoms are considerably larger than the experimental value of bulk Fe. Cluster calculations for Fe metal with the DV method[14] give a moment of $2.8\mu_B$, which is somewhat larger than the experimental value of $2.2\mu_B$ but still considerably smaller than the presently calculated value. Again, the increased moment on the NNN Fe atoms is due to the fact that these are surface atoms in the cluster and thus only partially bonded. The moments on the Ni atoms are somewhat higher than that for Ni metal. We conclude that the partial isolation of the Fe atoms, stacked as two-dimensional arrays, is the factor responsible for the increased magnetic moment of Fe atoms in FeNi, as compared to bulk iron.

We have calculated the contact hyperfine field at the nucleus of the central Fe atom in the following manner: the spin density of the valence electrons was obtained from the cluster calculation, and the $1s$, $2s$, and $3s$ spin densities were obtained from an atomic local-density calculation for the same value of $\alpha$. The hyperfine field is large and negative ($-244$ kOe); the valence contribution is positive ($+164$ kOe) and more than canceled by the negative terms of the core polarization. The theoretical value is in very good agreement with the value reported for meteoritic tetrataenite (288 kOe) and microcrystalline

TABLE IV. Mulliken populations and charges for the 19-atom cluster. NN denotes nearest neighbor; NNN denotes next-nearest neighbor.

| | Fe (center) | $Fe_{NN}$ | Ni | $Fe_{NNN}$ (axial) | $Fe_{NNN}$ (equatorial) |
|---|---|---|---|---|---|
| $3d$ | 6.68 | 6.60 | 8.70 | 6.45 | 6.48 |
| $4s$ | 0.50 | 0.75 | 0.83 | 0.97 | 1.08 |
| $4p$ | 0.40 | 0.59 | 0.60 | 0.52 | 0.43 |
| Charge | 0.43 | 0.06 | $-0.12$ | 0.06 | 0.01 |
| Magnetic moment ($\mu_B$) | 3.33 | 3.40 | 0.79 | 3.98 | 3.76 |

material produced by neutron irradiation (288 kOe, 327 kOe). The magnetic properties of several Fe-Ni alloys have been investigated in another work.[18] From general experience, we conclude that the present calculated value of $H_f$ is uncertain by $\pm 50$ kOe due to our approximate treatment of core contributions and fundamental limitations of the local-density theory used here.


## ACKNOWLEDGMENTS

This work was supported by the Conselho Nacional de Desenvolvimento Científico e Tecnológico (CNPq, Brasil) and by the U.S. National Science Foundation, Grant No. INT83-12863. The authors thank Professor Jacques Danon for interesting discussions.


---

*Permanent address: Department of Physics and Astronomy, Northwestern University, Evanston, IL 60201.


[1]R. S. Clarke, Jr. and E. R. D. Scott, Am. Mineral. **65**, 624 (1980).

[2]J. F. Albertsen, Phys. Scr. **23**, 301 (1981).

[3]J. Paulevé, D. Dautreppe, J. Laugier, and L. Néel, C. R. Acad. Sci. Paris **254**, 965 (1962).

[4]A. D. Romig, Jr. and J. I. Goldstein, Metall. Trans. **A11**, 1151 (1980); C. E. Johnson, M. S. Ridout, and T. E. Cranshaw, Proc. Phys. Soc. London **81**, 1079 (1963); U. Gonser, S. Nasu, and W. Kappes, J. Magn. Magn. Mater. **10**, 244 (1979).

[5]Y. Gros and J. Paulevé, J. Phys. (Paris) **31**, 459 (1970).

[6]J. Danon, R. B. Scorzelli, I. Souza Azevedo, J. Laugier, and A. Chamberod, Nature (London) **284**, 537 (1980).

[7]R. B. Scorzelli, Ph.D. thesis, University of Paris, 1985 (unpublished).

[8]D. E. Ellis, Int. J. Quantum Chem. **S2**, 35 (1968); D. E. Ellis and G. S. Painter, Phys. Rev. B **2**, 2887 (1970); A. Rosén, D. E. Ellis, H. Adachi, and F. W. Averill, J. Chem. Phys. **85**, 3629 (1976).

[9]J. C. Slater, *The Self-Consistent Field for Molecules and Solids*, Vol. 4 of *Quantum Theory of Molecules and Solids* (McGraw-Hill, New York, 1974).

[10]A. H. Stroud, *Approximate Calculation of Multiple Integrals* (Prentice-Hall, Englewood Cliffs, NJ, 1971).

[11]G. A. Benesh and D. E. Ellis, Phys. Rev. B **24**, 1603 (1981).

[12]N. N. Greenwood and T. C. Gibb, *Mössbauer Spectroscopy* (Chapman and Hall, London, 1971).

[13]D. Guenzburger and D. E. Ellis, Phys. Rev. B **22**, 4203 (1980).

[14]D. Guenzburger and D. E. Ellis, Phys. Rev. B **31**, 93 (1985).

[15]S. N. Ray and T. P. Das, Phys. Rev. B **16**, 4794 (1977).

[16]R. E. Watson and L. H. Bennett, Phys. Rev. B **18**, 6439 (1978).

[17]D. E. Ellis and D. Guenzburger, Phys. Rev. B **31**, 1514 (1985).

[18]D. Guenzburger, D. E. Ellis, and J. Danon, J. Magn. Magn. Mater. **59**, 189 (1986).